SUPPORTING INFORMATION

EVALUATION OF GELATIN-BASED HYDROGELS FOR COLON AND PANCREAS STUDIES USING 3D *IN VITRO* CELL CULTURE

Regina Pamplona [†], Sandra González-Lana [‡,§], Ignacio Ochoa [§,‖,⊥], Rafael Martín-Rapún [,†,‖,#], and Carlos Sánchez-Somolinos [*,‖,¶]*

[†] Aragón Institute of Nanoscience and Materials (INMA), CSIC-University of Zaragoza, Department of Organic Chemistry, C/ Pedro Cerbuna 12, 50009 Zaragoza, Spain

[‡] BEONCHIP S.L., CEMINEM, Campus Río Ebro. C/ Mariano Esquillor Gómez s/n, 50018 Zaragoza, Spain

[§] Tissue Microenvironment (TME) Lab. Aragón Institute of Engineering Research (I3A), University of Zaragoza, C/ Mariano Esquillor s/n, 500018 Zaragoza, Spain

[‖] CIBER in Bioengineering, Biomaterials and Nanomedicine (CIBER-BBN), Madrid, Spain

[⊥] Institute for Health Research Aragón (IIS Aragón), Paseo de Isabel La Católica 1-3, 50009 Zaragoza, Spain

[#] Universidad de Zaragoza, Facultad de Ciencias, Departamento de Química Orgánica, C/ Pedro Cerbuna 12, 50009 Zaragoza, Spain

[¶] Aragón Institute of Nanoscience and Materials (INMA), CSIC-University of Zaragoza, Department of Condensed Matter Physics (Faculty of Science), C/ Pedro Cerbuna 12, 50009 Zaragoza, Spain

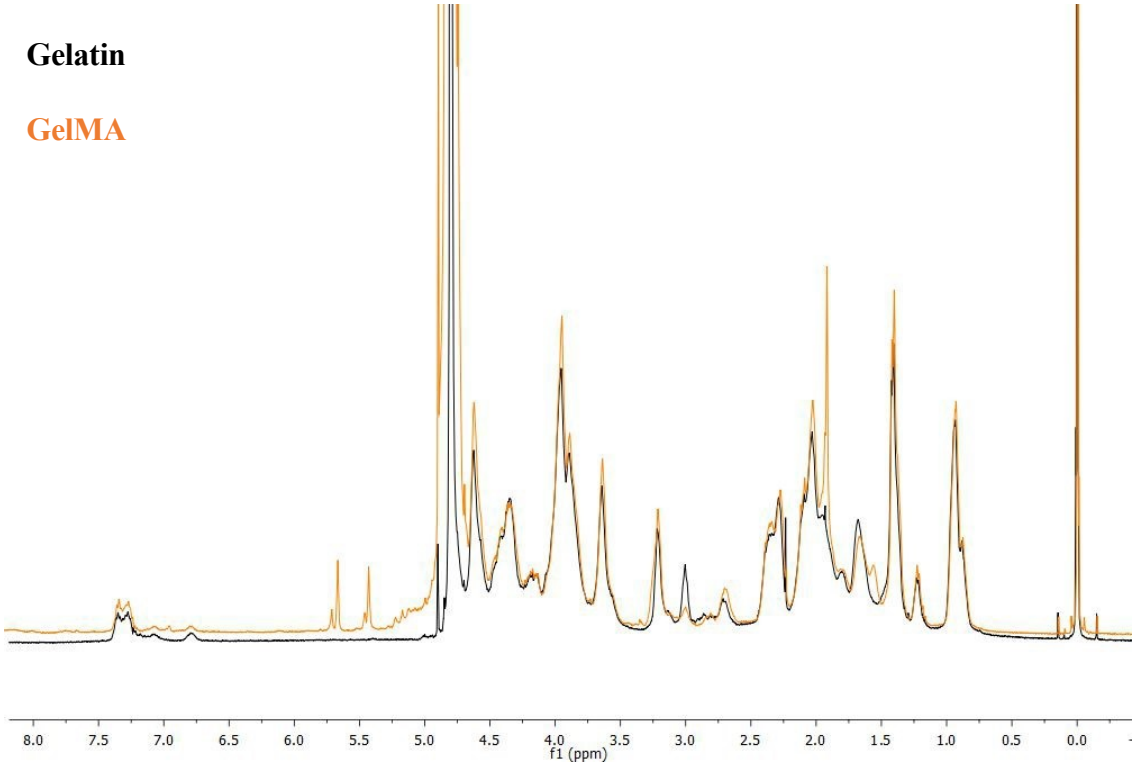

Figure S1. ^{1}H-NMR spectra of commercial gelatin (black line) and synthesized GelMA (orange line). The emergence of methacrylamide proton bands at 5.58 and 5.35 ppm, along with a significant reduction in the band at 2.91 ppm (corresponding to unmodified lysine ε-CH2), can be attributed to the functionalization of gelatin.

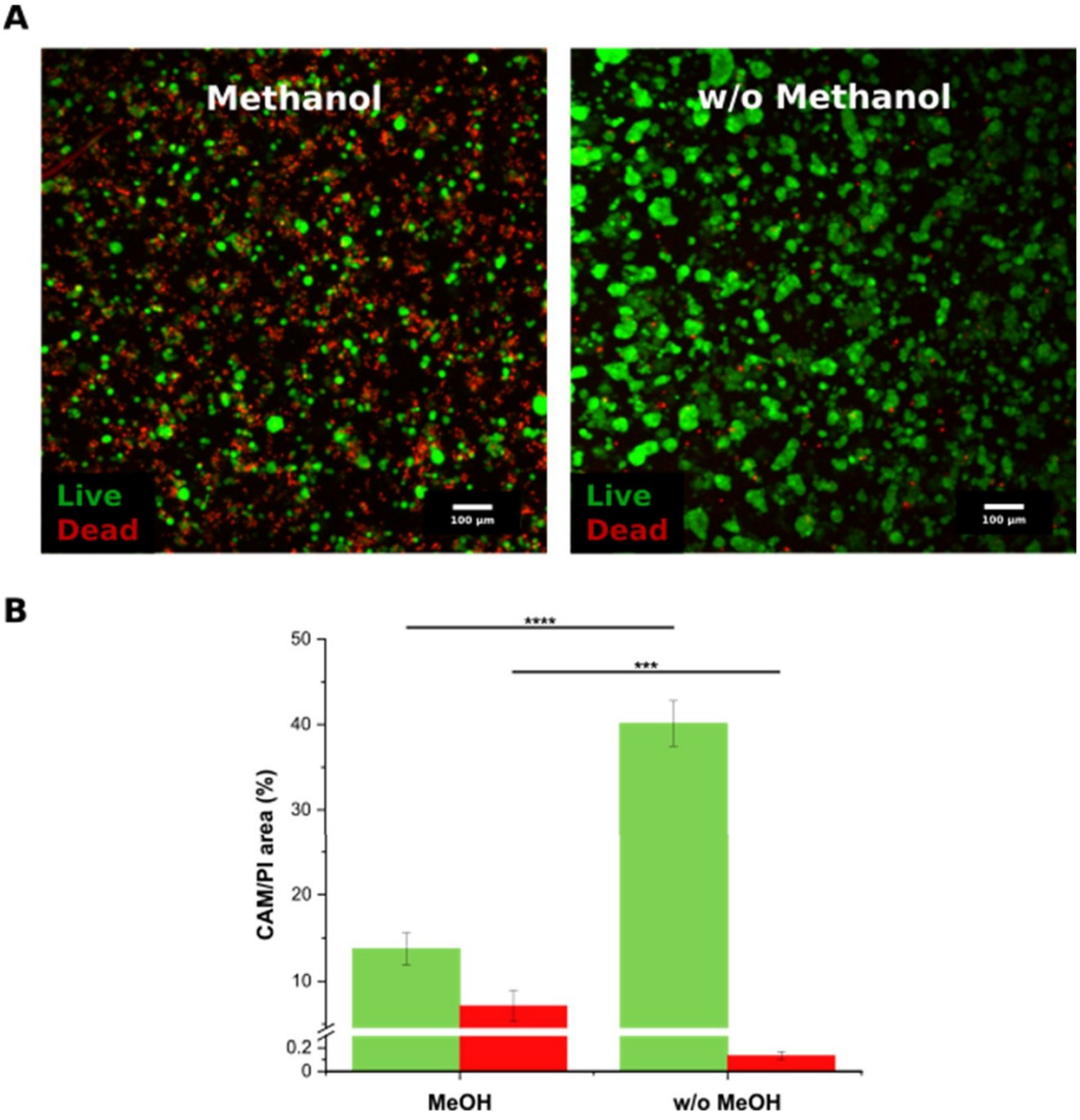

Figure S2. Effect of methanol on cell viability of HCT-116 cells embedded within GelMA-150 hydrogels. A) Live/Dead micrographs of HCT-116 cells embedded within GelMA-150 hydrogel after 24 h of cell culture containing methanol (left) or without methanol (right) in the initial photoinitiator solution. B) Area percentage of alive CAM (green) and dead PI (red) stained cells from micrographs of HCT- cells on GelMA-150 scaffolds on day-1. Error bars SD. Note: ****$p < 0.0001$, ***$p < 0.001$.

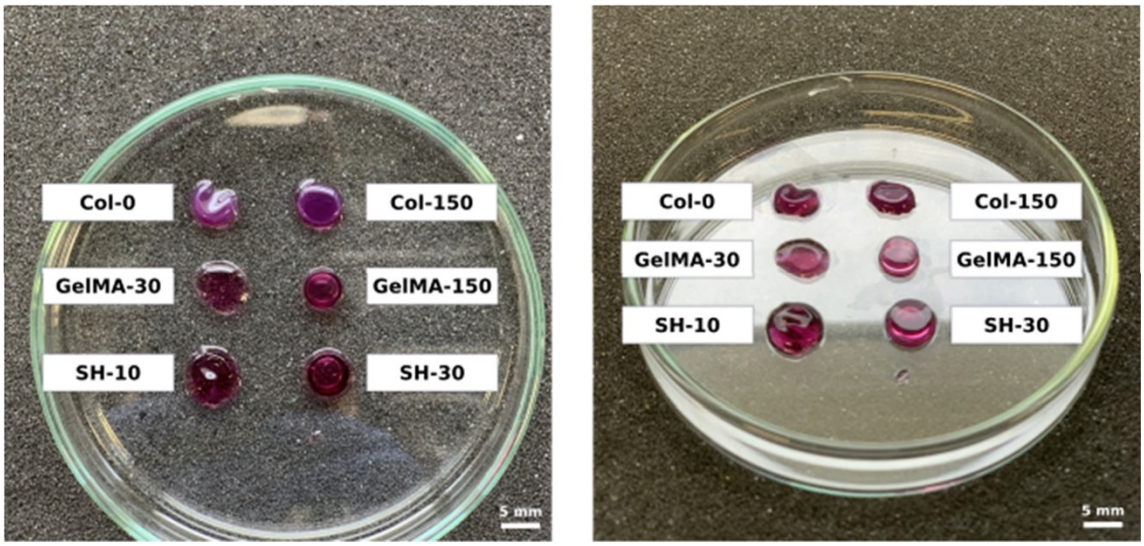

Figure S3. Cell-free hydrogels stained after MTS assay.

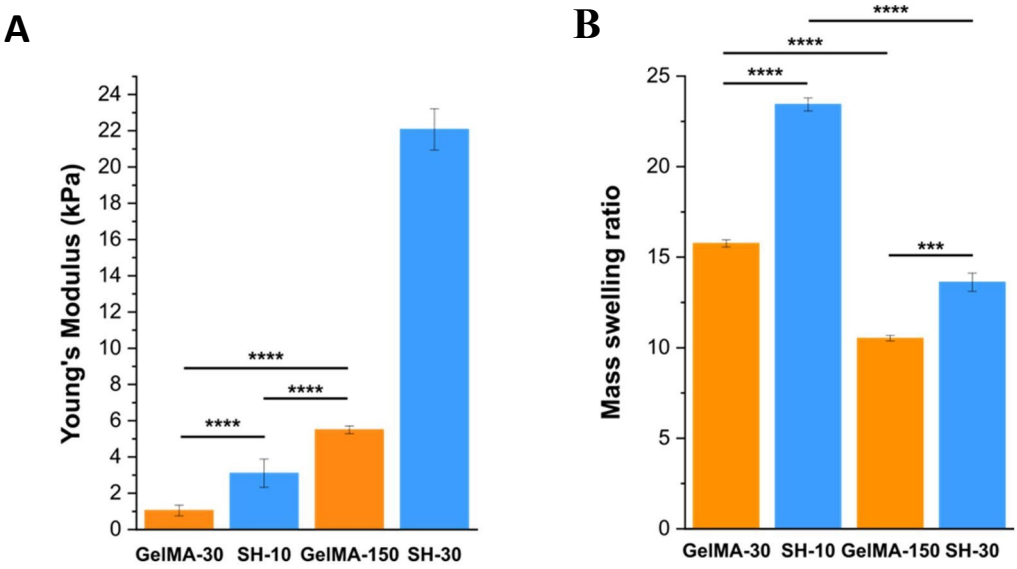

Figure S4. Mechanical characterization in terms of stiffness (A) and mass swelling ratio (B) of methanol-formulated GelMA-30, SH-10, GelMA-150 and SH-30 hydrogels (extracted from Ref. 17). Error bars SD. Note: ****p < 0.0001, ***p < 0.001. Non-statistical differences are not drawn in the graph.

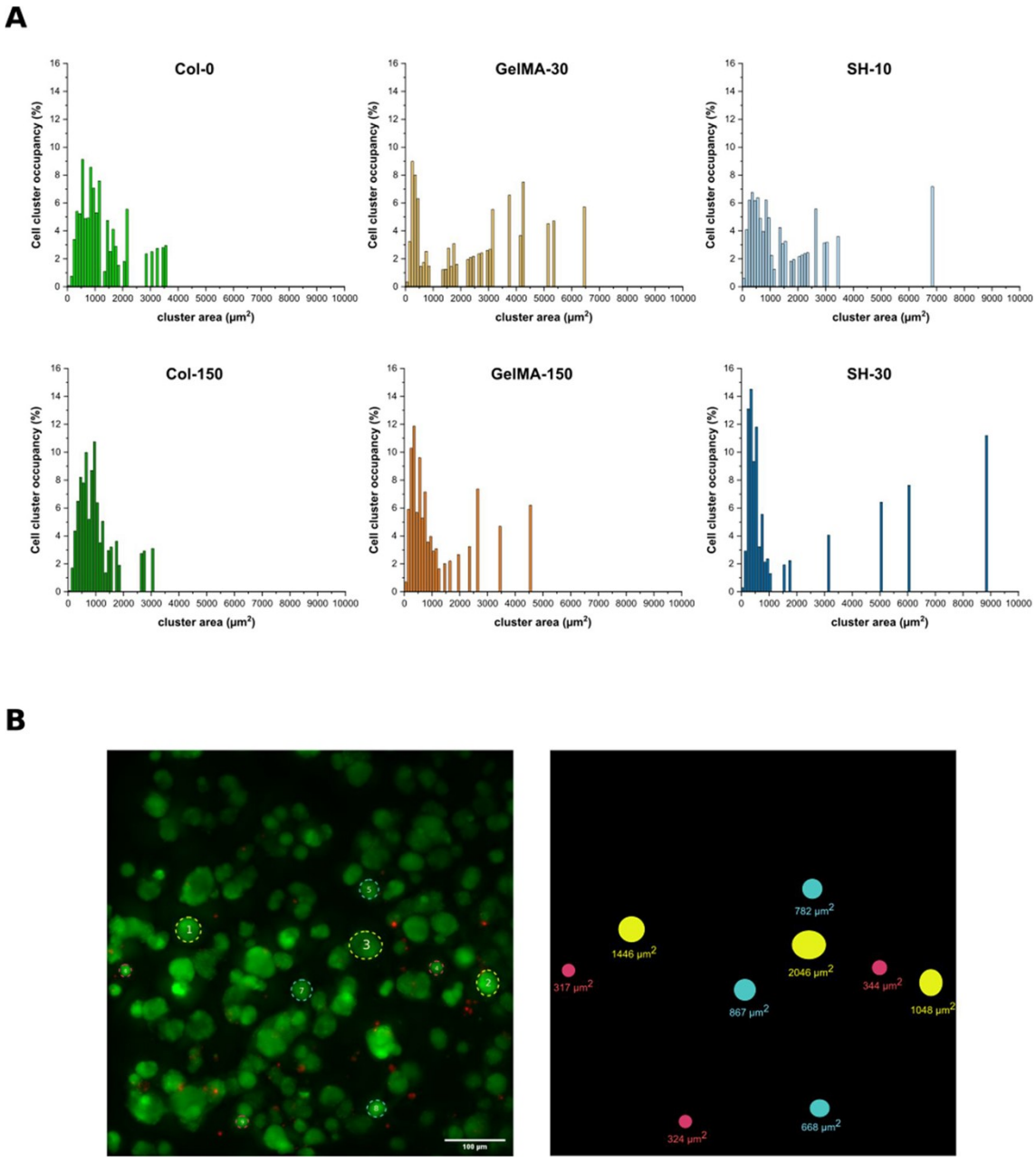

Figure S5. HCT-116 cluster size analysis after 3 days of 3D cell culture. A) Histograms of cell cluster occupancy percentage (over total cluster area) depending on the cell cluster area for collagen and GelMA-based hydrogels on day-3. B) Visual scheme on cluster size quantification. Clusters were manually thresholded to spheroidal or ovoid shapes and classified into three categories: smaller than 500 μm^2 (pink), medium size from 500 to 1000 μm^2 (blue) or larger than 1000 μm^2 (yellow).

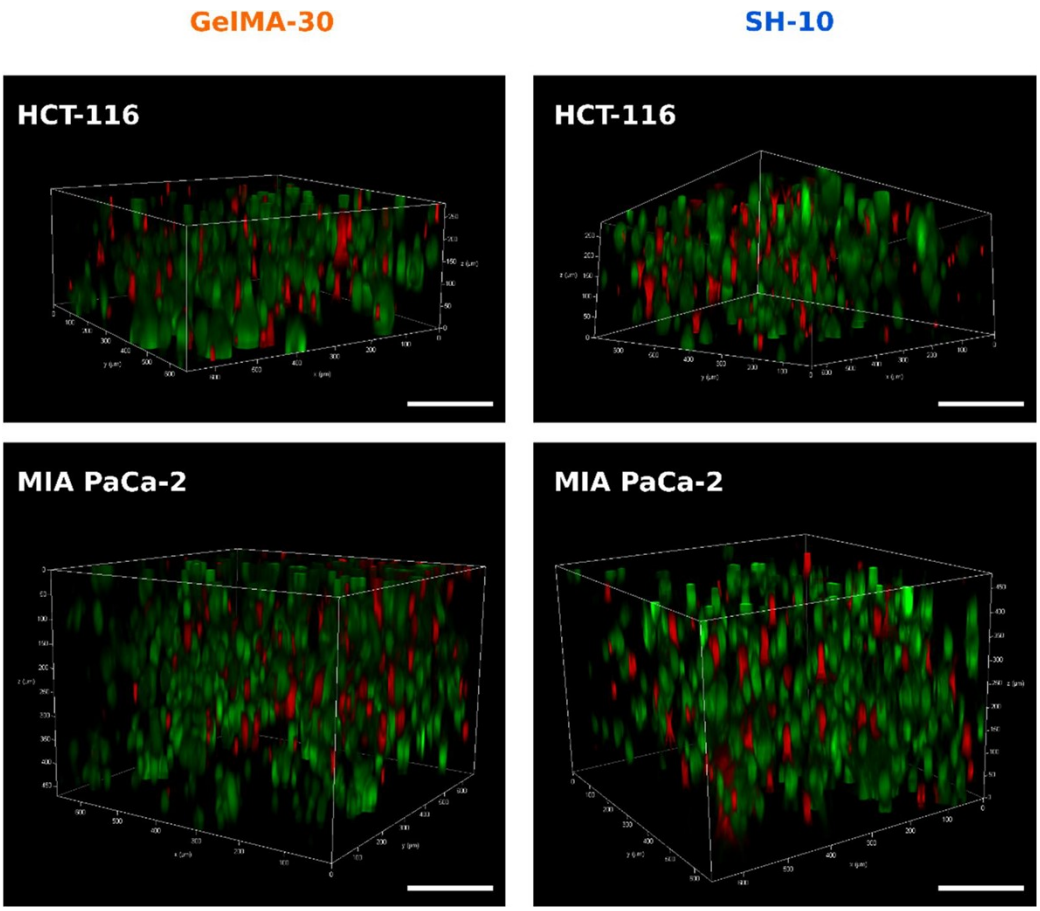

Figure S6. 3D renders of Live/Dead micrographs showing the three-dimensional distribution of HCT-116 cells (above) and MIA PaCa-2 cells (below) within GelMA-30 and SH-10 hydrogels after 3 days of 3D cell culture. 3D renders corresponding to HCT-116 and MIA PaCa-2 cells measure 650x650x270 µm and 650x650x470 µm, respectively. The scale bar represents 200 µm.

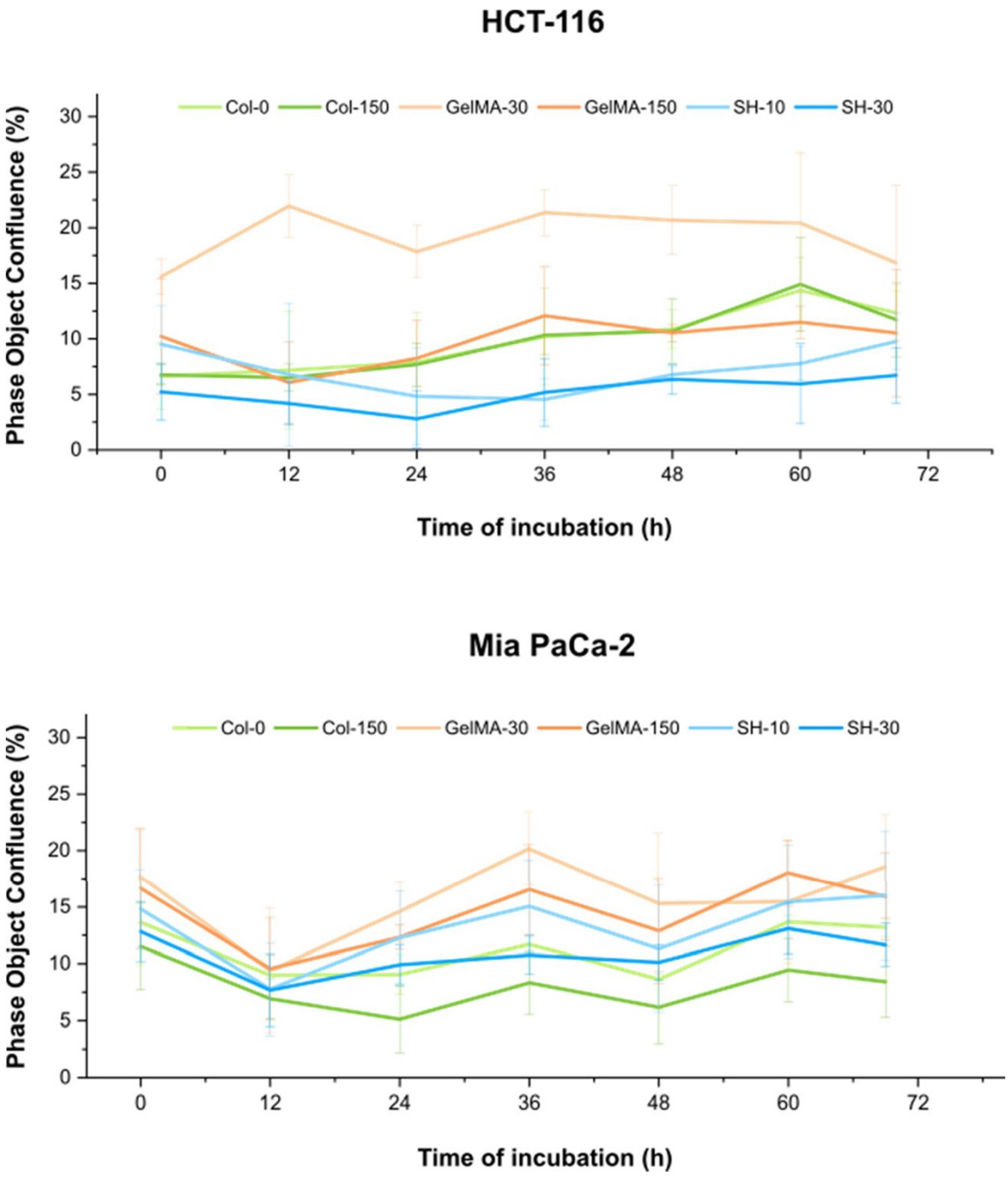

Figure S7. Phase object confluence percentage as a function of time of incubation for collagen and GelMA-based hydrogels embedded with HCT-116 (upper) and MIA PaCa-2 (lower) cells. Error bars SD.

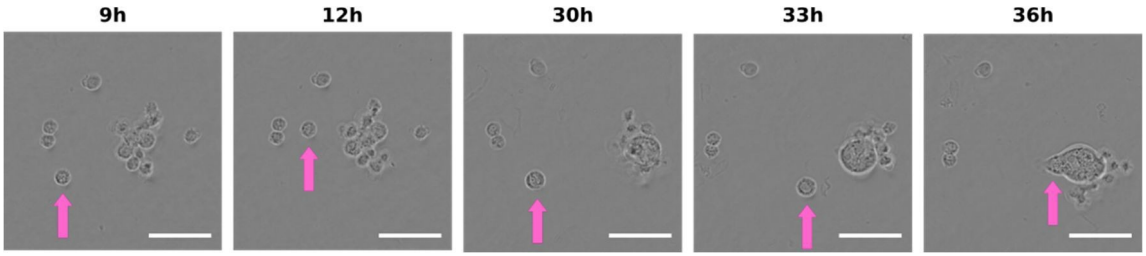

Figure S8. Phase-contrast images from IncuCyte® experiment showing **individual migration** (pink arrows) of single HCT-116 cells in GelMA-30 hydrogel over time. The scale bar represents 50 µm for 20X micrographs.

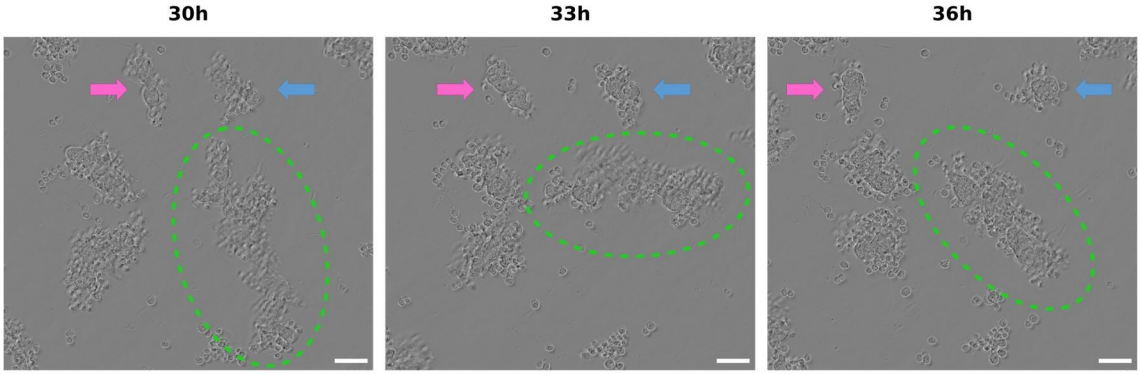

Figure S9. Phase-contrast images from IncuCyte® experiment showing HCT-116 **clusters migration** (pink and blue arrows) and **rotation** in (dashed green line) SH-10 hydrogel. The scale bar represents 50 µm for 20X micrographs.

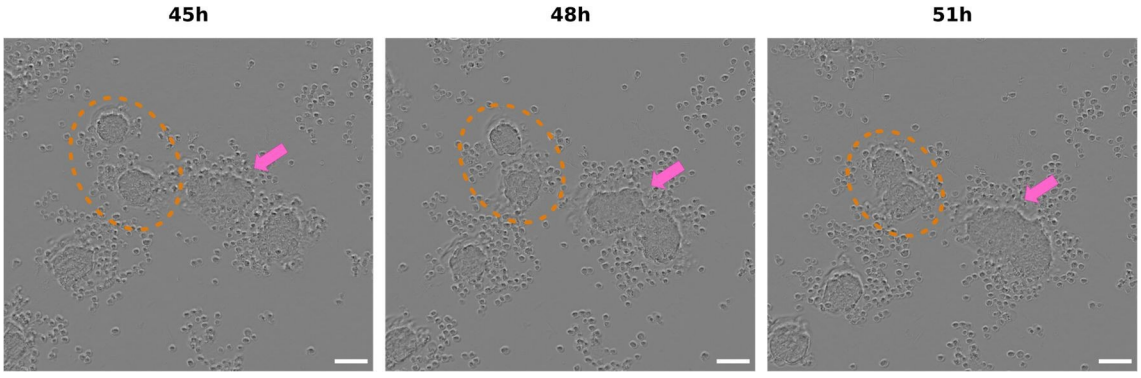

Figure S10. Phase-contrast images from IncuCyte® experiment showing HCT-116 clusters approximation to form a **larger aggregate** (pink arrows and dashed orange line) in SH-10 hydrogel. The scale bar represents 50 µm for 20X micrographs.

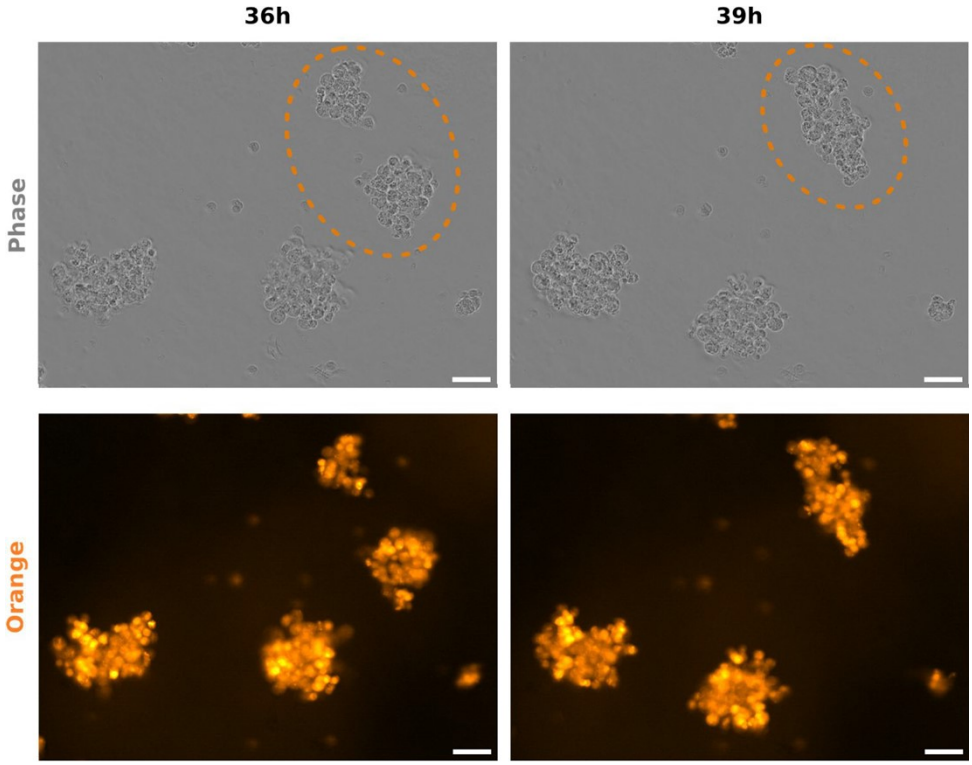

Figure S11. Phase-contrast and orange fluorescence images from IncuCyte® experiment showing **migration** of MIA PaCa-2 groups of cells (dashed orange line). The scale bar represents 50 μm for 20X micrographs.

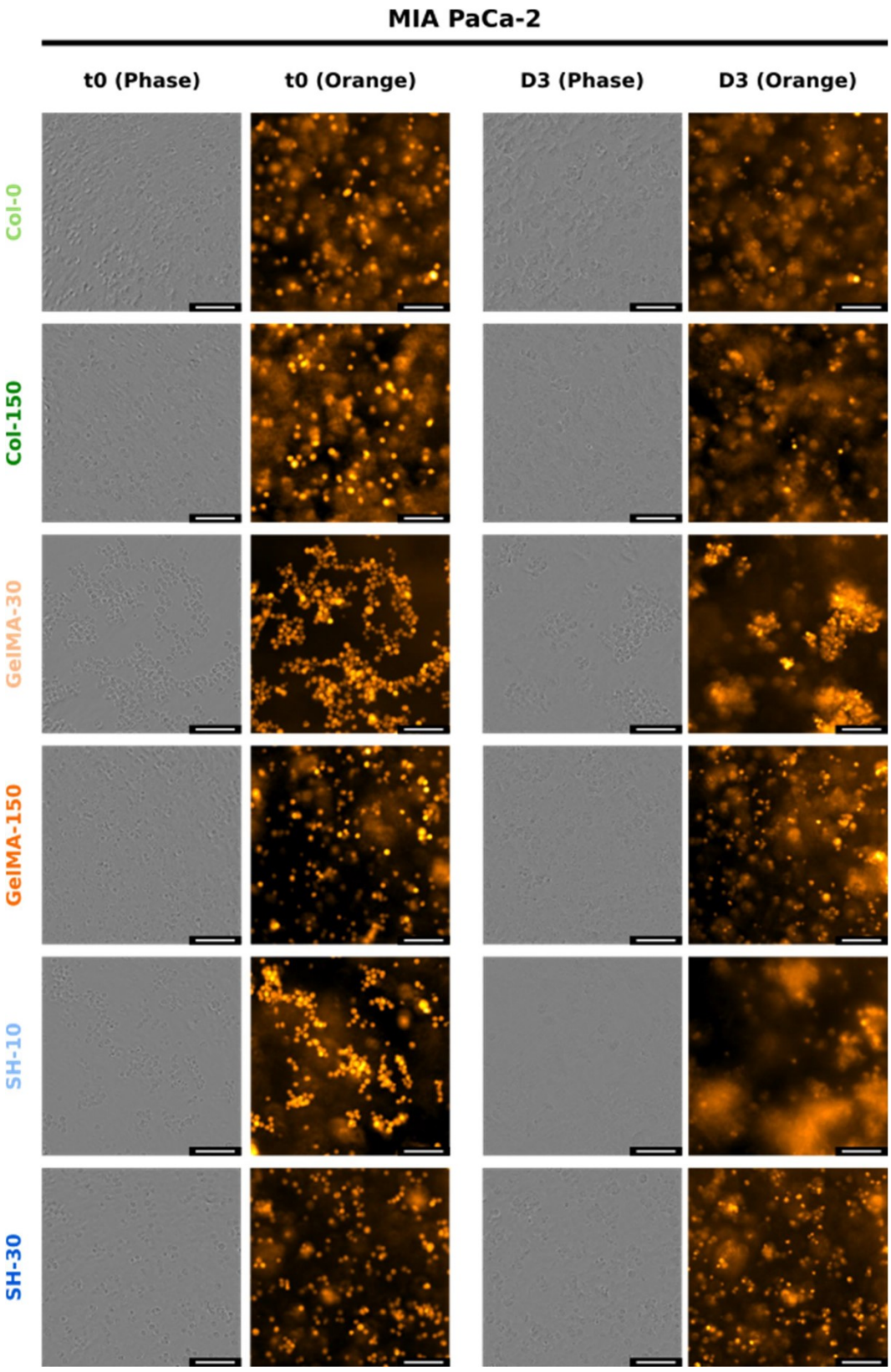

Figure S12. Phase-contrast and orange fluorescence images from IncuCyte® of MIA PaCa-2-embedded hydrogels at t=0 (left) and day-3 (right) . The scale bar represents 100 µm for 20X micrographs.

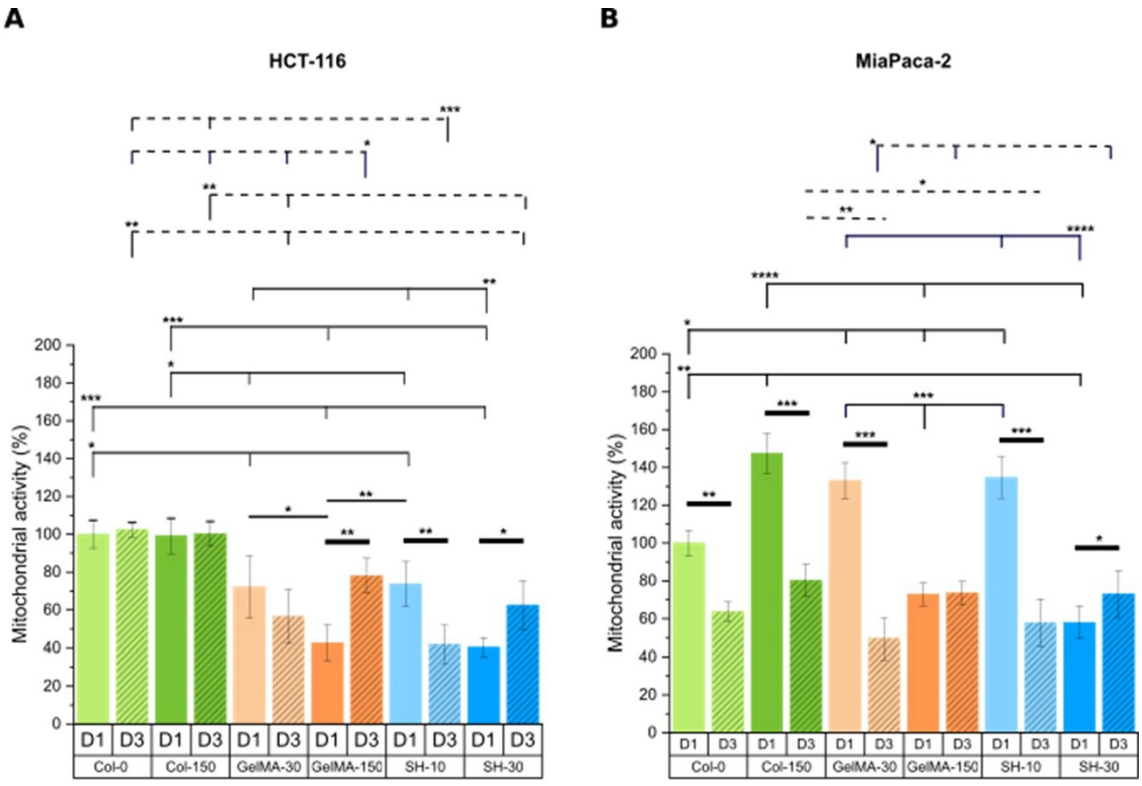

Figure S13. Complete statistical analysis from MTS assay to determine mitochondrial metabolic activity for hydrogels embedded with HCT-116 (A) and MIA PaCa-2 cells (B) on day-1 and day-3. Error bars SD. Note: ****$p < 0.0001$, ***$p < 0.001$, **$p < 0.01$, *$p < 0.05$. Thin and dashed lines represent statistics among scaffolds on day-1 and day-3, respectively. Thick lines correspond to statistical differences between day-1 and day-3 within the same condition. (Non-statistical differences are not drawn in the graph).

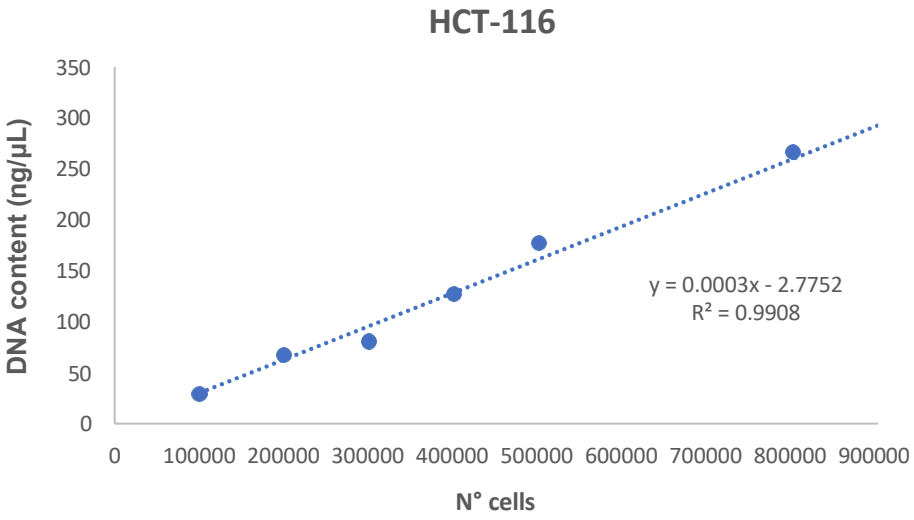

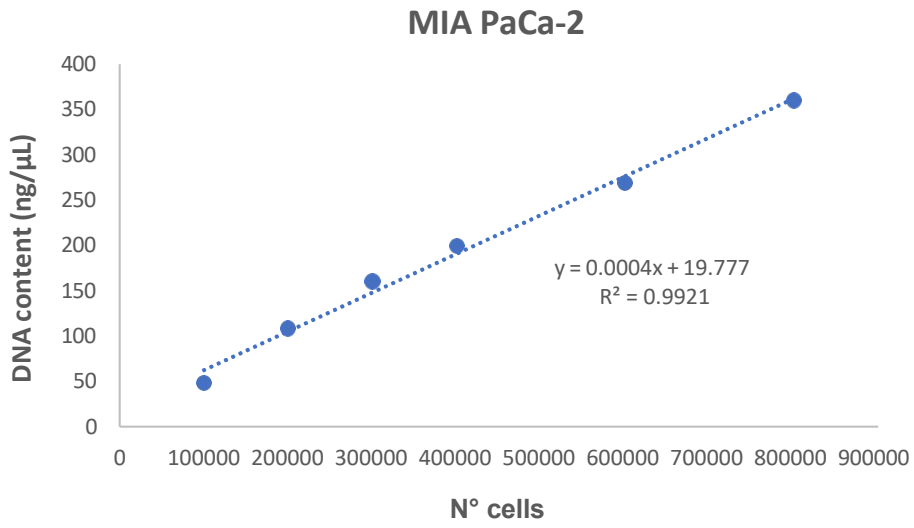

Figure S14. HCT-116 (above) and MIA PaCa-2 (below) calibration curves for DNA quantification with increasing cell concentrations from 100000 to 800000 cells.

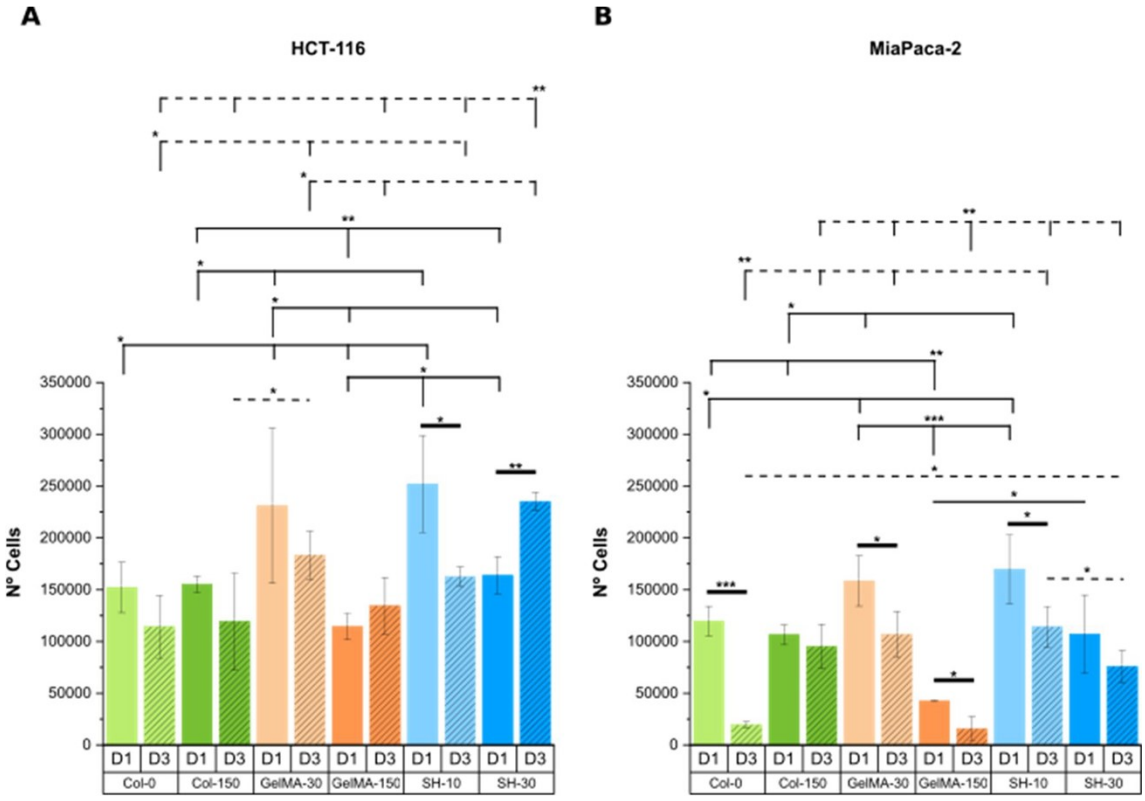

Figure S15. Complete statistical analysis from DNA extraction to determine the number of HCT-116 (A) and MIA PaCa-2 cells (B) embedded within collagen and GelMA-based hydrogels on day-1 and day-3. Error bars SD. Note: ****p < 0.0001, ***p < 0.001, **p < 0.01, *p < 0.05. Thin and dashed lines represent statistics among scaffolds on day-1 and day-3, respectively. Thick lines correspond to statistical differences between day-1 and day-3 within the same condition. (Non-statistical differences are not drawn in the graph).